Optical Spectra of Cu(II)−Azurin by Hybrid TDDFT-Molecular Dynamics Simulations

Michele Cascella, Michel A. Cuendet, Ivano Tavernelli, and Ursula Rothlisberger*

Laboratory of Computational Chemistry and Biochemistry, Ecole Polytechnique Fédérale de Lausanne (EPFL), FSB-ISIC-BCH 4109 1015, Lausanne, Switzerland

Received: March 9, 2007; In Final Form: May 15, 2007

The ground state electronic structure of oxidized azurin from *Pseudomonas aeruginosa* and its optical response have been investigated by combining hybrid quantum mechanics/molecular mechanics simulations with time-dependent density functional theory. In agreement with experiment, we find that the unpaired electron spin density is mainly localized on the copper ion. The vertical absorption spectrum in the visible range is well reproduced, with the central band centered around 2.1 eV. The anisotropic dipolar field due to the extended α-helix polarizes the metal binding site and is responsible for a shift of the absorption bands by ±0.1−0.2 eV. At 300 K, the bond distances of the copper binding site undergo large fluctuations (∼0.3 Å). It is crucial to take these thermal fluctuations into account for a faithful description of the optical properties.

1. Introduction

Metal ions are ubiquitously present in biological systems in the form of counterions or as active centers of metalloproteins and ribozymes. In fact, in these systems, tailored metal centers fine-tune the chemical and optical properties for fundamental life processes, such as proteolysis, respiration or cellular signaling.[1−3] Some metal centers host transition metal ions that are optically active in the visible range and thus open the possibility to serve as sensitive optical probes for an exploration of their surrounding biochemical environment.[4]

In the present work, we have investigated the electronic and excited-state properties of metalloproteins in the prototypical case of the electron-transfer (ET) protein azurin from *Pesudomonas aeruginosa*.[5] We have chosen this system in view of the fact that metalloproteins involved in ET processes constitute a particularly interesting class for electronic structure-based theoretical predictions. In fact, their biological function is directly related to the electronic structure of the metal itself, which is, in turn, strongly coupled to the surrounding protein matrix.[2,6,7] Azurin belongs to the single-copper cupredoxin family, also known as *blue copper proteins* (BCPs). BCPs are particularly appealing for theoretical studies, due to their relatively small size and the great availability of experimental measurements in the literature. BCPs exchange electrons among themselves or with other redox proteins, such as cytochrome c551 or nitrite reductase, using a protein-bound Cu metal ion, that can exist in the Cu(II) or Cu(I) redox states.[6,8] The protein−metal interactions evolved to tune the redox and optical properties of copper, which greatly differ from those of the copper complexes in solution. In fact, the protein environment influences the properties of the metal center through the ligand field created by the closeby residues, through the long-range electrostatic potential, and through modulation of the structural and vibrational properties of the protein−metal complex via the imposition of mechanical constraints. The copper ion forms a type-1 Cu binding site (Figure 1), which is characterized by a bright blue color, a narrow hyperfine splitting in the Electron Paramagnetic Resonance (EPR) spectra, a high reduction potential,[9−11] and a strong structural similarity between oxidized and reduced states.[9−15] In fact, in both oxidation states, the copper ion is coordinated by a cysteine (Cys) thiolate group and two histidine (His) nitrogen atoms in a trigonal planar geometry. The coordination polyhedron is completed by one axial ligand, typically a methionine (Met) thioether group. In azurin, a backbone amide oxygen of a glycine (Gly) constitutes an additional axial ligand.[5]

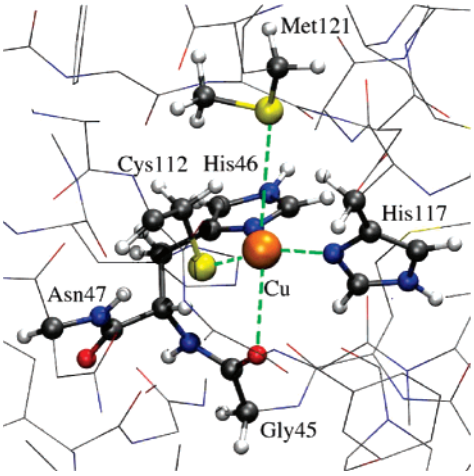

Figure 1. Copper binding site of azurin. The QM atoms are represented in balls-and-sticks, and neighboring MM atoms are drawn in lines. The rest of the system is not drawn for simplicity.

During the last decades, different quantum chemistry studies have addressed cluster models of BCP copper binding sites,[16−21] elucidating different aspects of their electronic structure. In particular, they have evidenced a prevalently covalent character of the Cu−planar ligand interactions (in particular, with the Cys112 sulfur atom), and a relatively large delocalization of the unpaired electron density in the oxidized form of the metal−protein complex. However, experimental studies on azurin from pseudomoas areuginosa[22,23] and plastocyanin from Anabaena variabilis (A.c. PCu)[24] suggest a stronger localization of the unpaired electron on Cu than that proposed by cluster calculations. Recent independent studies on three different BCPs

* Address correspondence to this author. Phone: +41-(0)21-6930321. Fax: +41-(0)21-6930320. E-mail: ursula.roethlisberger@epfl.ch.

10.1021/jp071938i CCC: $37.00
Published on Web 08/03/2007

(plastocyanins, rusticyanin,[25] and azurin[7]) have shown that the electrostatic field produced by the protein frame directly influences their redox properties. Finally, recent studies[26,27] have shown that thermal fluctuations significantly affect biological ET rates.

In recent years, Density Functional Theory (DFT) based computer simulations have provided a reliable description of structural and dynamical properties of the ground state of different proteins complexed to various metal ions, e.g., zinc and copper.[28,29] In addition, time-dependent DFT (TDDFT)[30] has emerged as a promising framework to describe excited-state properties of a variety of systems, from solid-state nanomaterials to organic chromophores bound to proteins.[31−35] Although major failures of TDDFT, e.g., photoexcitation associated to cis−trans isomerizations or charge-transfer phenomena, are known,[36,37] typical metal-to-ligand excitations are known to be in good agreement with experiments,[38−40] therefore, suggesting TDDFT as a reliable tool for characterization of the optical properties of metal centers in proteins.

In the present work, we have performed a study of the electronic structure and excitation spectra of the oxidized form of azurin by means of hybrid QM/MM Car−Parrinello molecular dynamics simulations (MD)[41,42] in combination with TDDFT. We have addressed the sensitivity of the localization of the unpaired spin density with respect to different parameters, like the use of different exchange/correlation (XC) functionals, different QM/MM partitioning, geometrical strain, finite temperature effects, and different spin density assignment criteria. In summary, we find that the unpaired electron is more localized on copper than on the sulfur atom of Cys112, in agreement with experiments.[22,23] TDDFT, in this case, provides a very good description of the optical properties of the system, which are influenced by the long-range electrostatic field and are directly coupled to the thermal motion of the protein frame.

2. Computational Details

In our computational setup, the protein was solvated by 8648 water molecules in a 69 × 61 × 67 Å^3 orthorhombic periodic box. The copper ion, its direct ligands and the backbone of Asn47, which is H-bonded to the sulfur atom of Cys112, were described at the spin-polarized DFT level by using the PBE[43] and BLYP[44,45] XC functionals (see Figure 1). The rest of the protein and the solvent were treated at the classical mechanics level with the Amber force field (parm98[46]). Core−valence interactions were integrated out via norm-conserving Martins−Troullier pseudopotentials;[47] the electronic wave functions were expanded in plane waves up to a cutoff of 70 Ry. The interaction between the classical and the quantum part was described via a fully-Hamiltonian hierarchical coupling scheme.[42] Initially, the system was relaxed starting from the crystal structure (PDB code 4AZU[5]) by 2 ns of classical molecular dynamics, keeping the copper center close to the crystal structure by using positional harmonic restraints. Then, the classical Hamiltonian was substituted by the QM/MM one, and the energy of the system was carefully minimized by repeated cycles of simulated annealing. Subsequently, the system was heated to 300 K starting from an initial temperature of 50 K within 2 ps of MD. Our QM/MM setup, based on the pre-equilibrated classical MD structure, was able to converge to equilibrated structural and dynamical features of the binding site that were stable all along the 8 ps of QM/MM simulation (with an average rmsd of 0.34 Å from the crystal structure). Configurations sampled every 0.5 ps along the run were used to average the electron spin localization and the optical spectra. The effect of self-interaction corrections (SIC) was tested by a SIC implementation[48] that uses a weighted form of the Perdew Zunger (PZ)[49] correction to GGA functionals. An empirical coefficient λ is introduced to scale the orbital dependent PZ potential:

$$V_i^{\mathrm{PZ},\sigma} = -\lambda \int \frac{\rho_i^{\sigma}(r')}{|r-r'|}\,\mathrm{d}r' - V_{\mathrm{XC}}^{\mathrm{GGA},\sigma}[\rho_i^{\sigma},0] \qquad (1)$$

According to the unrestricted formulation of Kohn Sham-DFT, ρ_i^{σ} corresponds to the density of a spin population in the *i*th orbital. The best fit for the parameter λ was obtained for a training set made of organic radicals, and was found to be 0.35.

The absorption spectrum of the Cu(II)−azurin system was calculated by linear-response TDDFT[30] (GGA/PBE[43]) within the Tamm−Dancoff approximation.[50]

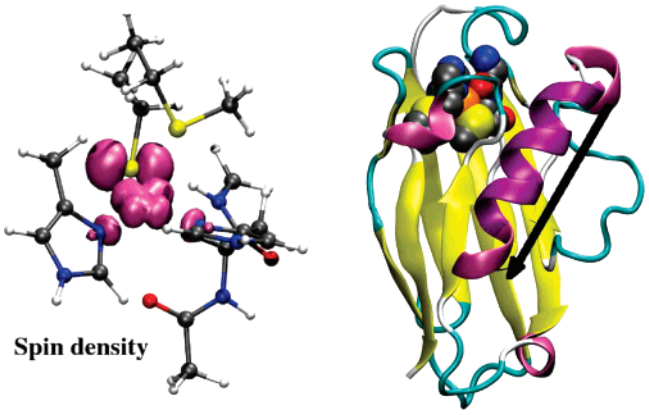

Figure 2. Distribution of the unpaired spin density at the binding site of azurin. Left: The electron spin density is drawn in mauve; MM atoms are not drawn for clarity. Right: Structure of azurin. The atoms of the copper binding site are drawn in spheres. The cartoon representation of the protein indicates the secondary structure elements. The black arrow specifies the direction of the electrostatic dipole produced by the α-helix.

3. Results and Discussion

Spin Density Localization. A first characteristic electronic property of the copper binding site is the distribution of the unpaired spin density. Assignment of the spin density to the atoms of the systems has been done by direct spatial integration of the Voroni cells. Our unrestricted DFT calculations show that the spin density is localized on the $d_{x^2-y^2}$ orbital of the Cu ion as well as on the planar ligands (see Figure 2, left panel), a finding that is in qualitative agreement with previously reported cluster[16,18,19] and QM/MM calculations on plastocyanin.[21] Both PBE and BLYP predictions are in good qualitative agreement with model fits from different ENDOR experiments on azurin[22,23] and EPR measurement on plastocyanin,[24] which despite the relatively large uncertainty (e.g., ±20% for ref 22) show that the spin density should be more localized on the copper ion than on sulfur. Inclusion of self-interaction corrections to the DFT Hamiltonian[48,49] further increases the spin density localization on Cu with respect to S.

In contrast, former quantum chemical studies based on cluster models of the binding site[16,18,19]and QM/MM calculations,[21] using Mulliken population analysis to assign atomic spin densities, have suggested a relatively large delocalization of the unpaired electron density onto the ligands (e.g., about 50% of the spin density on Cys112). To give a rationale for this discrepancy, we have probed the sensitivity of our data for both PBE and BLYP functionals with respect to the QM size of our setup, as well as to other parameters, such as the electrostatic

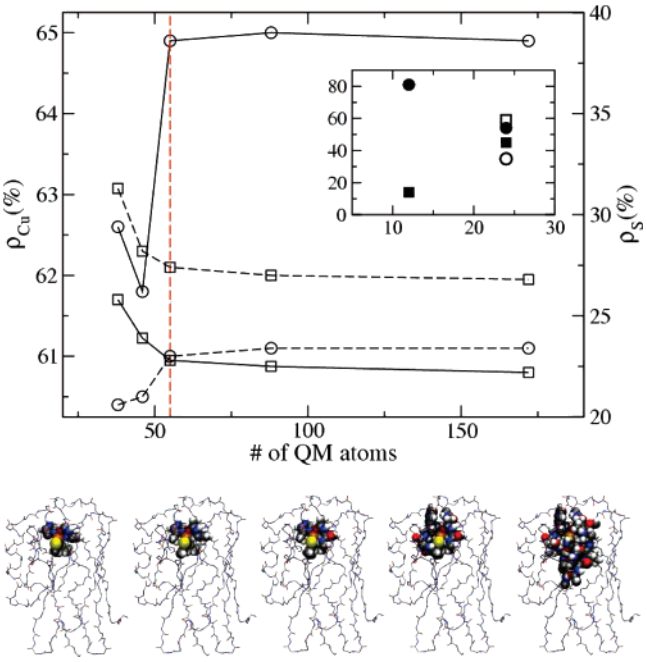

Figure 3. Unpaired spin density localization on Cu (ρ_{Cu}, ○) and Cys112-S atoms (ρ_S, □) as a function of the number of QM atoms (PBE XC functional[43]). Main graph: Data points connected by a straight line (−) refer to QM/MM calculations and those by a dashed line (---) refer to cluster calculations. After inclusion of the Asn47 backbone in the QM part (red dashed line) data stabilizes around a nearly constant and size independent value. Inset: Data from ref 16 (filled symbols) and ref 19 (blank symbols). Bottom panels: QM/MM partitions considered in the plot. The QM atoms are drawn in spheres and the backbone of the MM part of the protein in lines.

coupling to the surrounding region, to geometrical strain and finte temperature effects, and to the spin-density assignment criteria. Starting from a minimal system that only treats the copper ion and its first ligands at the QM level, we have progressively added neighboring shells of atoms, up to a size of 170 QM atoms. The plot in Figure 3, which reports the distribution of the unpaired spin density as a function of the number of QM atoms, suggests that the discrepancies found with respect to previously reported values of the spin density can partially be attributed to the small size of the investigated cluster models. Data of the localization of the unpaired spin density converge only after inclusion of the His46-Asn47 backbone, which forms a direct H-bond to the sulfur atom of Cys112 (Figure 1), and which is considered to be relevant for the functionality of azurin.[51] Different theoretical and experimental studies have indicated the strong influence that H-bonds have to metal-bound sulfur atoms in different systems,[52−59] thus confirming the importance of this moiety for a correct description of the electronic properties of this binding site. This is particularly important in view of the fact that the CASSCF data of ref 16 are based on $Cu(SH)(H_2S)(NH_3)_2^+$ and $Cu(SH)(H_2)(imidazole)_2^+$ models of the active site, while the MRD-CI data of ref 19 refer to a $Cu(CH_3S)(imidazole)_2^+$ cluster. These models are much smaller than the convergence threshold indicated in Figure 3. The effect of the rest of the protein is purely electrostatic, and its description at the classical level is sufficiently accurate. In fact, any further increase of the QM region does not affect our data (Figure 3). To quantify the importance of the long-range electrostatic coupling on the spin polarization, we have repeated single point calculations for all the QM parts in Figure 3 in vacuo. In all cases, we observe a decrease of the localization of the spin density on the copper ion (up to 4%), independent of the size of the QM cluster considered. A similar trend has been recently found in QM/MM calculations of plastocyanin.[21] Geometrical strain also influences the spin localization. In fact, cluster calculations with nonrelaxed geometries taken directly from the X-ray structure result in a decrease of about 7% of the total spin-density on the copper ion with respect to data from cluster calculations on the fully relaxed QM/MM geometries (see Table 1). On the other hand, variations of the spin density for structures sampled during QM/MM MD runs at room temperature are never larger than 2%. Therefore, thermal effects do not dramatically affect this property. Finally, a possible source of uncertainty in theoretical prediction of the spin density distribution can originate from the different assignment methods used (e.g., Mulliken population analysis vs. spatial intregration). In fact, projection onto a minimal atomic orbital basis followed by a Mulliken population analysis leads to assignments of 50.9% and 27.8% of the total spin density to copper and sulfur, respectively, for the PBE functional (that is, a discrepancy up to 15% with respect to the values obtained from direct spatial integration). A similar trend has been found for the BLYP functional (42.3% and 38.1% for Cu and S, respectively, compared to 52.4% and 34.7% from spatial integration). It is relevant to note that, in the case of azurin, the nodal surface of the spin density is such that a spatial assignment to the atoms is straightforward (see Figure 2). Therefore, direct spatial integration of the spin density should provide more accurate results than estimates based on a Mulliken population analysis.

Optical Absorption. Vertical transitions from the electronic ground state have been initially computed for eight different configurations, spaced at 1 ps intervals along the QM/MM MD run. Then, convergence has been checked by doubling the number of the sampled structures, and by comparing the results with those obtained by another set of structures originating from a second fully independent QM/MM MD run (structures available in the Supporting Information). The average standard deviation of the vertical absorption energies sampled for different configurations of the QM/MM run is ∼0.15 eV, which causes the broad shape of the absorption band (Figure 4). Sampling of the ground-state configurations at finite temperature is essential to obtain convergence of the optical bands. At 300

TABLE 1: Computed Upaired Spin Density Localization (in %)[a]

	cluster (X-ray)		QM/MM				exptl	
atoms	PBE	BLYP	PBE	BLYP	PBE-SIC	BLYP-SIC	ref 22	ref 23
Cu	67.8	54.9	64.9 (50.9)	52.4	77.6	71.6	60	45
S_{Cys112}	22.1	31.9	22.5 (27.8)	34.7	15.1	19.9		30
$N_{\delta,His46}$	3.1	3.3	3.8 (4.0)	4.0	3.3	3.9	4.9	
$N_{\delta,His117}$	3.0	3.5	4.3 (5.0)	4.5	4.0	5.0	9.4	

[a] Cluster calculations with identical size QM region based on the non-relaxed X-ray structure, and MD-averaged QM/MM calculations are presented. Data refer to PBE and BLYP GGA-exchange/correlation functionals; (-SIC) suffix labels data including self-interaction correction. For all data, spatial integration of the spin-density has been used,while data in parentheses for QM/MM-PBE refer to assignments with Mulliken population analysis.

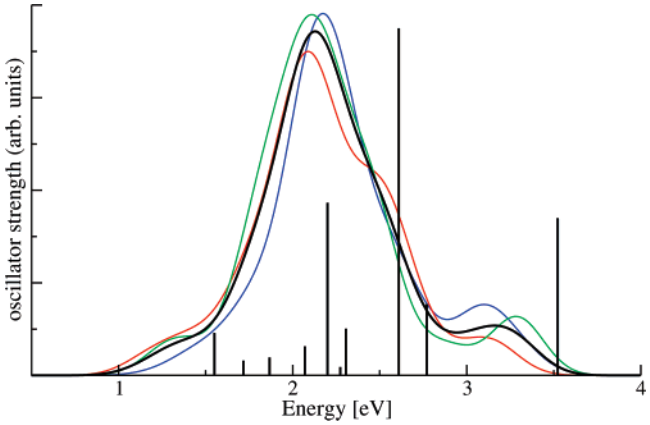

Figure 4. Convergence of the optical spectrum. The black line is the averaged spectrum. The red, green, and blue lines correspond to the three different sets of structures, as discussed in the text. The vertical bars represent the transitions obtained from one, arbitrarily chosen, single snapshot during QM/MM MD.

K, the atomic distances of the binding site undergo large fluctuations (the standard deviation of the Cu−axial ligand bond lengths is, e.g., ∼0.3 Å). It turns out that the photoabsorption bands are highly sensitive to the geometry of the copper center. In fact, the absorbtions of neither of the single configurations alone are able to reproduce satisfactorily the experimental spectrum (Figure 4).[60] The spectrum shows an intense absorption in the yellow-green region, with two bands centered at 2.1 and 2.5 eV, and a broad absorption in the near-IR to red, with a band centered at 1.5 eV, and a peak at 3.1 eV, leading to the typical blue color of azurin solutions. Absorption in the blue-violet region, on the other hand, is relatively weak. The agreement with experimental data is very good[61] especially if we consider the relatively small number of structures used for the sampling. The major deviation from the experimental data consists of a relative blue shift (by 0.2−0.3 eV) of the two higher energy bands that are more sensitive to sampling issues.

We have characterized the absorption bands via an analysis in terms of Kohn−Sham orbitals (KSO). KSO and energies of the two spin states become very different when approaching the frontier levels. The *singly occupied molecular orbital*, that is, the Kohn Sham level that is formally the HOMO for the β-spin states, is about 1.4 eV lower in energy for the β population. The nine highest occupied KSOs are very close in energy, and their ordering can vary with thermal fluctuations of the structure. The absorption bands in the visible spectrum are associated with a strong response of the α-spin states, with only a negligible contribution from the β electron manifold. All the optical transitions have a strong mixed character. The lowest energy absorption band localizes the hole predominantly on a π orbital between the Cys112 sulfur atom and the $d_{x^2-y^2}$ Cu orbital, while, for the two more intense bands in the yellow-green region, the hole is shared by states characterized by different contributions from copper $d_{xz/yz}$ orbitals and Cys112 sulfur p orbitals. The low intensity absorptions in the blue-violet region share the hole between the π system of His46 or His117, as well as $d_{xz/yz}$ orbitals of the copper ion (Figure 5). The excited electron is always localized on the α-LUMO orbital, which shows an antibonding character between the $d_{x^2-y^2}$ copper orbital and the planar ligands, in particular, a p orbital of the S atom. This KSO has the same symmetry as the ground-state electron spin density (Figure 2). These findings are in good agreement with experiments[6,61] and CASPT2 model calculations.[16] The nature of the optical transitions provides also a rationale for the good performance of TDDFT for this system. In fact, all

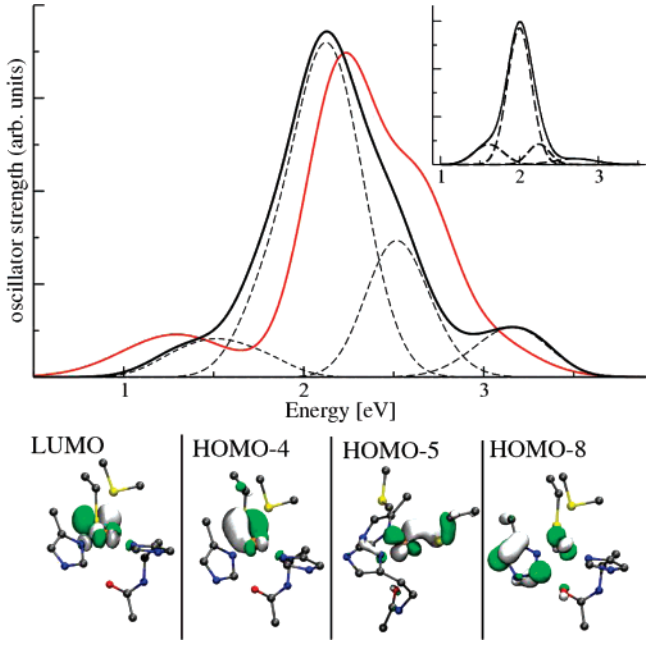

Figure 5. Absorption spectrum of Cu(II)−azurin. Top panel: The black line is the computed TDDFT-spectrum. A Gaussian decomposition of the spectrum, corresponding to tentative band assignments, is given as dashed lines. Red line: TDDFT-spectrum neglecting the electrostatic coupling to the MM part of the system. Right inset: Experimental spectrum.[61] Bottom panels: Kohn−Sham wave functions for the α-spin states dominantly involved in the electronic excitations (HOMO-4 to LUMO: lower energy band; HOMO-5 to LUMO: central bands; HOMO-8 to LUMO: higher energy band).

transitions imply the response of the electron density localized around a few atoms, and have a minimal charge-transfer character, also reported in ref 16, that is one of the principal potential sources of errors in TDDFT calculations. To probe the importance of the coupling between the external electric field of the protein and the optical response of the copper binding site, we have repeated the spectra calculations without the presence of the protein external field. In this case, we have observed a change in the relative energies of the KSOs, and a nontrivial modification of their TDDFT response, with a red-shift of the low-energy and high-energy bands by ∼0.2 eV and a blue-shift of the central bands by ∼0.1 eV (Figure 5). These shifts relate to the electrostatic field anisotropy along the *z* axis in the binding site (thus, almost perpendicular to the $d_{x^2-y^2}$-Cu and His π-orbitals, and parallel to $d_{xz/yz}$-Cu ones), for which the dipolar contribution of the α-helix (the only one present in the azurin structure, Figure 2) at 9 Å distance from the copper center is dominant.

4. Concluding Remarks

Our study shows that a combined QM/MM-TDDFT strategy is able to reproduce the characteristic features of the electronic structure of the binding site of a copper metalloprotein in its ground and excited states. The strongly coupled metal−protein system provides a sensitive test for electronic structure methods. The electron spin density is a particularly sensitive quantity. In fact, the use of different XC functionals and different assignment criteria can lead to values ranging from 42.3% to 64.9% of the total spin-density on the copper ion. Using direct spatial integration, we find that in any case the spin-density is more localized on the copper ion than on the sulfur atom of Cys112, in agreement with experiments.[22,23] Thermal fluctuations of the molecular structure and electrostatic coupling

between the metal center and the surrounding protein modulate the electronic properties of the system; therefore, a reliable description of such susceptible quantities as the electron spin density distribution and the optical response can be achieved only by taking these effects explicitly into account. These factors also play an important role for the determination of other electronic properties of these systems, such as their particular redox potentials and low reorganization energies[7,25] which ensure fast ET rates and are crucial for the in vivo functionality of ET-proteins.[51]

Acknowledgment. This investigation has been supported by the Swiss National Science Foundation. Computations have been performed on the IBM-BlueGene Supercomputer at EPFL. The authors wish to thank Dr. Alessandra Magistrato and Dr. Ute F. Röhrig for enlightening discussions.

Supporting Information Available: Sampled structures. This material is available free of charge via the Internet at http://pubs.acs.org.

References and Notes

(1) Berg, J. M.; Stryer, L.; Tymoczko, J. L. *Biochemistry*, 5th ed.; Freeman: New York, 2002.
(2) Gray, H. B.; Winkler, J. R. *Proc. Natl. Acad. Sci. U.S.A.* **2005**, *102*, 3534−3539.
(3) Barondeau, D. P.; Getzoff, E. D. *Curr. Op. Struct. Biol.* **2004**, *14*, 765−774.
(4) Bertini, I.; Gray, H. B.; Lippard, S. J.; Valentine, J. S. *Bioinorganic Chemistry*; University Science Books: Mill Valley, CA, 1994.
(5) Nar, H.; Messerschmidt, A.; Huber, R.; van de Kamp, M.; Canters, G. W. *J. Mol. Biol.* **1991**, *221*, 765−772.
(6) Penfield, K. W.; Gewirth, A. A.; Solomon, E. I. *J. Am. Chem. Soc.* **1985**, *107*, 4519−4529.
(7) Cascella, M.; Magistrato, A.; Tavernelli, I.; Carloni, P.; Rothlisberger, U. *Proc. Natl. Acad. Sci. U.S.A.* **2006**, *103*, 19641−19646.
(8) Solomon, E. I.; Lowery, M. D. *Science* **1993**, *259*, 1575−1581.
(9) Skyes, A. G. *Adv. Inorg. Chem.* **1991**, *36*.
(10) Adman, T. *Adv. Prot. Chem.* **1991**, *42*.
(11) Messerschmidt, A. *Struct. Bonding* **1998**, *90*.
(12) Colman, P. M.; Freeman, H. C.; Guss, J. M.; Murata, M.; Norris, V. A.; Ramshaw, J. A. M.; Venkatappa, M. P. *Nature* **1978**, *272*, 319−324.
(13) Guss, J. M.; Freeman, H. C. *J. Mol. Biol.* **1983**, *169*, 521−563.
(14) Shepard, W. E. B.; Anderson, B. F.; Lewandoski, D. A.; Norris, G. E.; Backer, E. N. *J. Am. Chem. Soc.* **1990**, *112*, 7817−7819.
(15) DiBilio, A. J.; Hill, M. G.; Bonader, N.; Karlsson, B. G.; Villahermosa, R. M.; G.Malmström, B.; Winkler, J. R.; Gray, H. B. *J. Am. Chem. Soc.* **1997**, *119*, 9921−9922.
(16) Pierloot, K.; de Kerpel, J. O. A.; Ryde, U.; Ollson, M. H. M.; Roos, B. O. *J. Am. Chem. Soc.* **1998**, *120*, 13156−13166.
(17) Ryde, U.; Olsson, M. H. M. *Int. J. Quantum Chem.* **2001**, *81*, 335−347.
(18) Jaszewski, A. R.; Jezierska, J. *Chem. Phys. Lett.* **2001**, *343*, 571−580.
(19) van Gastel, M.; Coremans, J. W. A.; Sommerdijk, H.; Hemert, M. C.; Groenen, E. J. J. *J. Am. Chem. Soc.* **2002**, *124*, 2035−2041.
(20) Corni, S. *J. Phys. Chem. B* **2005**, *109*, 3423−3430.
(21) Sinnecker, S.; Neese, F. *J. Comp. Chem.* **2006**, *27*, 1463−1475.
(22) Coremans, J. W. A.; Poluektov, O. G.; Groenen, E. J. J.; Canter, G. W.; Nar, H.; Messerschmidt, A. *J. Am. Chem. Soc.* **1996**, *118*, 12141−12153.
(23) Fittipaldi, M.; Warmerdam, G. C. M.; deWaal, E. C.; Canters, G. W.; Cavazzini, D.; Rossi, G. L.; Huber, M.; Groenen, E. *ChemPhysChem* **2006**, *7*, 1286−1293.
(24) Hansen, D. F.; Led, J. J. *J. Am. Chem. Soc.* **2004**, *126*, 1247−1252.
(25) Olsson, M. H. M.; Hong, G. Y.; Warshel, A. *J. Am. Chem. Soc.* **2003**, *125*, 5025−5039.
(26) Skourtis, S. S.; Balabin, I. A.; Kawatsu, T.; Beratan, D. N. *Proc. Natl. Acad. Sci. U.S.A.* **2005**, *102*, 3552−3557.
(27) Hoffman, B. M.; Celis, L. M.; Cull, D. A.; Patel, A. D.; Seifert, J. L.; Wheeler, K. E.; Wang, J.; Yao, J.; Kurnikov, L. K.; Nocek, J. M. *Proc. Natl. Acad. Sci. U.S.A.* **2005**, *102*, 3564−3569.
(28) Dal Peraro, M.; Llarull, L. I.; Rothlisberger, U.; Vila, A. J.; Carloni, P. *J. Am. Chem. Soc.* **2004**, *126*, 12661−12668.
(29) Colombo, M.; Gossens, C.; Tavernelli, I.; Rothlisberger, U. *R. Soc.* 2006, Special Vol. WATOC 2005, 85−100.
(30) Runge, E.; Gross, E. K. U. *Phys. Rev. Lett.* **1984**, *52*, 997−1000.
(31) Sergi, A.; Gruning, M.; Ferrario, M.; Buda, F. *J. Phys. Chem. B* **2001**, *105*, 4386−4391.
(32) Marques, M. A. L.; López, X.; Varsano, D.; Castro, A.; Rubio, A. *Phys. Rev. Lett.* **2003**, *90*, 258101.
(33) Laino, T.; Nifosi, R.; Tozzini, V. *Chem. Phys.* **2004**, *298*, 17−28.
(34) Premvardhan, L. L.; Buda, F.; van der Horst, M. A.; Luhrs, D. C.; Hellingwerf, K. J.; van Grondelle, R. *J. Phys. Chem. B* **2004**, *108*, 5138−5148.
(35) Amat, P.; Granucci, G.; Buda, F.; Persico, M.; Tozzini, V. *J. Phys. Chem. B* **2006**, *110*, 9348−9353.
(36) Tavernelli, I.; Rohrig, U. F.; Rothlisberger, U. *Mol. Phys.* **2005**, *103*, 963−981.
(37) Onida, G.; Reining, L.; Rubio, A. *Rev. Mod. Phys.* **2002**, *74*, 601−659.
(38) Monat, J. E.; Rodriguez, J. H.; McCusker, J. *J. Phys. Chem. A* **2002**, *106*, 7399−7406.
(39) Fantacci, S.; DeAngelis, F.; Selloni, A. *J. Am. Chem. Soc.* **2003**, *125*, 4381−4387.
(40) Chen, L. X.; Shaw, G. B.; Novozhilova, I. N.; Liu, T.; Jennings, G.; Attenkofer, K.; Mayer, G. J.; Coppens, P. *J. Am. Chem. Soc.* **2003**, *125*, 7022−7034.
(41) Car, R.; Parrinello, M. *Phys. Rev. Lett.* **1985**, *55*, 2471−2474.
(42) Laio, A.; VandeVondele, J.; Rothlisberger, U. *J. Chem. Phys.* **2002**, *116*, 6941−6948.
(43) Perdew, J. P.; Burke, K.; Ernzerhof, M. *Phys. Rev. Lett.* **1996**, *77*, 3865−3868.
(44) Becke, A. D. *Phys. Rev. A* **1988**, *38*, 3098−3100.
(45) Lee, C.; Yang, W.; Parr, R. G. *Phys. Rev. B* **1988**, *37*, 785−589.
(46) Cornell, W. D.; Cieplak, P.; Bayly, C. I.; Gould, I. R.; Caldwell, J. W.; Kollman, P. A. *J. Am. Chem. Soc.* **1995**, *117*, 5179−5197.
(47) Troullier, N.; Martins, J. L. *Phys. Rev. B* **1991**, *43*, 1993−2006.
(48) Tavernelli, I. Submitted for publication.
(49) Perdew, J. P.; Zunger, A. *Phys. Rev. B* **1981**, *23*, 5048−5079.
(50) Hutter, J. *J. Chem. Phys.* **2003**, *118*, 3928−3934.
(51) Zhuravleva, A. V.; Korzhnev, D. M.; Kupce, E.; Arseniev, A. S.; Billeter, M.; Orekhov, V. Y. *J. Mol. Biol.* **2004**, *342*, 1599−1611.
(52) Ayhan, M.; Xiao, Z. G.; Lavery, M. J.; Hamer, A. M.; Nugent, K. W.; Scrofani, S. D. B.; Guss, M.; Wedd, A. G. *Inorg. Chem.* **1996**, *35*, 5902−5911.
(53) Libeu, C. A. P.; Kukimoto, M.; Nishiyama, M.; Horinuchi, S.; Adman, E. T. *Biochemistry* **1997**, *36*, 13160−13179.
(54) Hall, J. F.; Kanbi, L. D.; Harvey, I.; Murphy, L. M.; Hasnain, S. S. *Biochemistry* **1998**, *37*, 11451−11458.
(55) Chen, K. S.; Tilley, G. J.; Sridhar, V.; Prasad, G. S.; Stout, C. D.; Armstrong, F. A.; Burgess, B. K. *J. Biol. Chem.* **1999**, *274*, 36749−36487.
(56) Low, D. W.; Hill, M. G. *J. Am. Chem. Soc.* **2000**, *122*, 11039−11040.
(57) Machczynski, M. C.; Gray, H. B.; Richards, J. H. *J. Inorg. Biochem.* **2002**, *88*, 375−380.
(58) Donaire, A.; Jimenez, B.; Fernandez, C. O.; Pierattelli, R.; Niizeki, T.; Moratal, J. M.; Hall, J. F.; Kohzuma, T.; Hasnain, S. S.; Vila, A. J. *J. Am. Chem. Soc.* **2002**, *124*, 13698−13708.
(59) Li, H.; Webb, S. P.; Ivanic, J.; Jensen, J. H. *J. Am. Chem. Soc.* **2004**, *126*, 8010−8019.
(60) This result can explain the fact that we find a better agreement with experiments than the one reported in the work of Sinnecker and Neese on plastocyanin,[21] where only the optimized structure is used.
(61) Solomon, E. I.; Hare, J. W.; Dooley, D. M.; Dawson, J. H.; Stephens, P. J.; Gray, H. B. *J. Am. Chem. Soc.* **1980**, *102*, 168−178.